Scientia Iranica A (2018) 25(4), 2000–2011

Sharif University of Technology
Scientia Iranica
Transactions A: Civil Engineering
http://scientiairanica.sharif.edu

Collocated Mixed Discrete Least Squares Meshless (CMDLSM) method for solving quadratic partial differential equations

S. Faraji Gargari[a], M. Kolahdoozan[a,*], and M.H. Afshar[b]

a. *Department of Civil & Environmental Engineering, Amirkabir University of Technology, 424, Hafez Ave., Tehran, P.O. Box 15875-4413, Iran.*
b. *School of Civil Engineering, Iran University of Science and Technology, Narmak, Tehran, P.O. Box 16846-13114, Iran.*

Received 6 September 2016; received in revised form 1 January 2017; accepted 4 February 2017

KEYWORDS
Meshless;
PDEs;
DLSM;
MDLSM;
Collocated points;
CMDLSM.

Abstract. In this paper, a collocated Mixed Discrete Least Squares Meshless (MDLSM) method is proposed and used to attain an efficient solution to engineering problems. Background mesh is not required in the MDLSM method; hence, the method is a truly meshless method. Nodal points are used in the MDLSM methods to construct the shape functions, while collocated points are used to form the least squares functional. In the original MDLSM method, the locations of the nodal points and collocated points are the same. In the proposed Collocated Mixed Discrete Least Squares Meshless (CMDLSM) method, a set of additional collocated points is introduced. It is expected that the accuracy of results may improve by using the additional collocated points. It is noted that the size of coefficient matrix is not increased in the proposed CMDLSM method compared with the MDLSM method. Therefore, the required computational effort for solving the linear algebraic system of equations is same as that in MDLSM method. A set of benchmark numerical examples, cited in the literature, is used to evaluate the performance of the proposed method. The results indicate that the accuracy of solutions is improved by using additional collocated points in the proposed CMDLSM method.

1. Introduction

Compared with mesh-based methods, Meshless methods are efficient alternatives for solving Partial Differential Equations (PDEs). Different versions of the mesh-based numerical methods, such as Finite Volume Method (FVM) [1] and Finite Element Method (FEM) [2], have been used for solving various engineering problems. A nonlocal finite element approach is presented and used for the simulation of nanobeams [3,4]. The convergence and stability property of nonlocal FEM method for the solution to elastoplasticity problem are also studied by a variational formulation [5]. Although the mesh-based methods are shown to be capable of accurately simulating the physical problems, these methods are faced with some difficulties when dealing with problems containing discontinuity and/or moving boundaries. These difficulties can be overcome or at least moderated by using meshless methods [6]. Although meshless methods are generally more efficient than standard FEM, they are generally more expensive and complicated [7]. Hence, some researchers have combined the FEM with

*. *Corresponding author. Tel.: +98 21 64543023; Fax: +98 21 64543023*
E-mail addresses: saebfaraji@aut.ac.ir (S. Faraji Gargari); mklhdzan@aut.ac.ir (M. Kolahdoozan); mhafshar@iust.ac.ir (M.H. Afshar)

doi: 10.24200/sci.2017.4203

the proper meshless methods to take advantage of the simplicity and computational efficiency of these methods [7]. Smoothed Finite Element Method (S-FEM) is one of the most well-known ones among these methods, which has been efficiently used for solving some engineering problems [8-10]. Recently, Mixed Discrete Least Squares Meshless (MDLSM) method, as a truly meshless method, was proposed and efficiently used to solve PDEs. In the current study, the concept of collocated points is introduced in MDLSM method, leading to Collocated Mixed Least Squares Meshless (CMLSM) method. Performance of the proposed method is then compared with the existing MDLSM method.

Unlike the mesh-based methods, only a set of nodes is used in meshless methods to discretize the domain. Therefore, time-consuming element-generation procedure is not needed in meshless methods. Furthermore, adaptive refinement procedures are conveniently carried out in meshless methods due to the fact that no element connectivity is required by them. In the last three decades, several meshless methods have been proposed and developed to solve PDEs. These methods are mainly categorized into two major classes regarding the approximation procedure: 1) Kernel function method; and 2) Polynomial series method. Smoothed Particle Hydrodynamics (SPH) and Moving Particle Semi-implicit (MPS) are the known meshless methods, which are based on the Kernel function method. The SPH method was primary proposed by Gingold and Monaghan (1977) and used for solving various fluid mechanics problems such as multiphase flows [11], free surface solid-fluid [12], and free surface flow in hydraulic structures [13] problems. In the MPS method, which is mainly similar to the SPH method, the partial spatial derivatives are calculated without using the gradient of Kernel function. This method has been successfully applied to solve free surface flow problem [14] and multi-phase flow problems [15]. Since the original MPS method did not ensure continuity of the first derivatives [14], a modified version of the method was presented [16]. Although the computational effort required for function approximation in the Kernel method is less than that in the polynomial series method, higher order consistency and accuracy can be obtained using the latter one [6].

Element-Free Galerkin (EFG) method is the most well-known method that uses the polynomial series approach. Several solid mechanics [17,18] and heat transfer [19] problems were efficiently solved by the EFG method. Since EFG uses the weak form of governing equations, the use of background mesh is unavoidable for numerical integration procedure. For this, the EFG method is not considered as a truly meshless method. Therefore, Meshless Local Petrov-Galerkin (MLPG) was proposed by Atluri and Zhu to alleviate the problem of background mesh in weak-form formulations. The method was used for simulating various solid [20] and fluid [21,22] mechanics problems. Although the problem of background mesh was overcome by the MLPG method, the method still suffered from a major drawback of asymmetric coefficient matrix and difficulties associated with the numerical integration procedure on and around the boundary nodes.

Another group of the meshless methods are also available, which use the strong form of the governing equations based on the collocation approach. SPH, Finite Point Method (FPM) [23-25], and Radial Point Interpolation Collocation Method (RPICM) are some of the meshless methods using the strong formulation [26-28]. Unlike the weak form, by using the strong form, the numerical integration procedure and the background mesh are not required. The strong form methods, however, may face the instability problem if the number and position of the collocation points are not suitably chosen. Therefore, several techniques have been proposed for improving the stability of the strong form methods, such as the upwind method used in the FPM when solving convection dominated problems [29]. The least-square technique used in LS-RPCM is shown to be a natural way to overcome the instability problems [30,31]. Since adaptive refinement procedures are simple and straightforward in the meshless methods based on the strong form, they are frequently combined with adaptive refinement algorithms [30-35].

The Discrete Least Squares Meshless (DLSM) method has recently been proposed by Afshar et al. (2006). Since it uses the strong-form governing equations, the method is considered as a truly meshless method. The DLSM method uses the Moving Least Squares (MLS) method as a polynomial series method to construct the shape functions. Since the method automatically leads to symmetric and positive-definite systems of equations irrespective of the problem type, it is not subjected to the Ladyzenskaja-Babuska-Brezzi (LBB) condition. The DLSM method was widely used to solve the linear elasticity mechanics [34,35] and free surface [36,37] problems. More recently, mixed formulation was used in the DLSM method, leading to the Mixed Discrete Least Squares Meshless (MDLSM) method [35,38,39] removing the need for time-consuming computation of the second derivatives of the MLS shape function. Furthermore, in the MDLSM method, the gradients are calculated more accurately than in the DLSM method [35,38,39]. More recently, the method was also used for solving the linear and non-linear propagation problems [40].

Firoozjaee and Afshar showed that the accuracy of DLSM method could be improved by using additional sampling points referee to collocated points [41]. In the current study, a set of additional collocated points is used in the MDLSM method; hence, the method is called Collocated Discrete Mixed Least Squares Meshless (CMDLSM) method. The additional collocated points are not used for function approximation and, therefore, do not change the size of the coefficient matrix. A series of benchmark problems, cited in the literature, is used to evaluate the performance of the proposed CMDLSM method in comparison with the MDLSM method and analytical solutions. Comparison of the results shows that the additional collocated points improve the accuracy of the proposed method.

2. Moving Least Squares (MLS) approximation

Various approximation and interpolation methods are used in meshless methods to construct the shape functions. In this section, the Moving Least Squares (MLS) approximation is presented briefly. More detailed explanation of the method is available in [38].

In MLS method, the unknown values ($u(\mathbf{X})$) are approximated by:

$$u(\mathbf{X}) = \mathbf{N}(\mathbf{X})\hat{\mathbf{u}}, \tag{1}$$

where $\mathbf{X}$ denotes the coordinate of collocated points and $\hat{\mathbf{u}}$ is the vector of nodal parameters defined by:

$$\hat{\mathbf{u}}^T = [\hat{u}_1, \hat{u}_2, ..., \hat{u}_{n_s}], \tag{2}$$

where n_s is the number of nodes in the support domain. The vector of MLS shape function ($\mathbf{N}(\mathbf{X})$) is defined as:

$$\mathbf{N}(\mathbf{X}) = \mathbf{P}^T(\mathbf{X})\mathbf{E}^{-1}(\mathbf{X})\mathbf{G}(\mathbf{X}), \tag{3}$$

where $\mathbf{E}(\mathbf{X})$ and $\mathbf{G}(\mathbf{X})$ are defined as follows:

$$\mathbf{E}(\mathbf{X}) = \sum_{j=1}^{n_s} \mathrm{w_j}(\mathbf{X} - \mathbf{X_j})\mathbf{P}(\mathbf{X_j})\mathbf{P}^{\mathrm{T}}(\mathbf{X_j}), \tag{4}$$

$$\mathbf{G}(\mathbf{X}) = [\mathrm{w}_1(\mathbf{X} - \mathbf{X}_1)\mathbf{P}(\mathbf{X}_1), \mathrm{w}_2(\mathbf{X} - \mathbf{X}_2)\mathbf{P}(\mathbf{X}_2), ..., \mathrm{w}_{n_s}(\mathbf{X} - \mathbf{X}_{n_s})\mathbf{P}(\mathbf{X}_{n_s})], \tag{5}$$

where w_j denotes the weight coefficient. In this study, a cubic spline weight function is used as follows:

$$\mathrm{w_j}(d) = \begin{cases} \frac{2}{3} - 4d^2 + 4d^3 & d \le \frac{1}{2} \\ \frac{4}{3} - 4d + 4d^2 - \frac{4}{3}d^3 & \frac{1}{2} \le d \le 1 \\ 0 \quad d \ge 1 \end{cases}$$

$$d = \|\mathbf{X} - \mathbf{X_j}\| / d_{wj}. \tag{6}$$

Here, d_{wj} defines the radius of the support domain at j-th node. The first order derivatives can be obtained by the following equations:

$$\frac{\partial \mathbf{N}}{\partial x} = \frac{\partial \mathbf{P}^T}{\partial x}\mathbf{E}^{-1}\mathbf{G} + \mathbf{P}^T\frac{\partial \mathbf{E}^{-1}}{\partial x}\mathbf{G} + \mathbf{P}^T\mathbf{E}^{-1}\frac{\partial \mathbf{G}}{\partial x}, \tag{7}$$

$$\frac{\partial \mathbf{N}}{\partial y} = \frac{\partial \mathbf{P}^T}{\partial y}\mathbf{E}^{-1}\mathbf{G} + \mathbf{P}^T\frac{\partial \mathbf{E}^{-1}}{\partial y}\mathbf{G} + \mathbf{P}^T\mathbf{E}^{-1}\frac{\partial \mathbf{G}}{\partial y}. \tag{8}$$

3. Collocated Mixed Discrete Least Squares Meshless (CMDLSM) method

Consider the following PDE as a typical quadratic equilibrium equation on a domain with the dimension of n_d:

$$\sum_{j=i}^{n_d}\sum_{i=1}^{n_d} a_{ij}\frac{\partial^2 T}{\partial x_{ij}^2} + \sum_{i=1}^{n_d} b_i\frac{\partial T}{\partial x_i} + cT = g, \qquad j \ge i, \tag{9}$$

subject to the following boundary conditions:

$$T(\mathbf{X}) = \bar{T}(\mathbf{X}),$$

$$\nabla T(\mathbf{X}) = \bar{\mathbf{q}}(\mathbf{X}), \tag{10}$$

where a_{ij}, b_i, and c denote the coefficients of governing PDE; $\bar{T}$ and $\bar{\mathbf{q}}$ are the prescribed Dirichlet and Neumann boundary conditions, respectively; and ∇ is the gradient operator.

In the mixed formulation, the first derivatives of the problem are primarily unknown and defined by:

$$\nabla T = \mathbf{q} = [q_1, q_2, ..., q_i, ..., q_{n_d}]. \tag{11}$$

$\mathbf{q}$ is considered as secondary unknown, which is computed simultaneously. Rewriting the governing equation along with the boundary conditions in terms of the new unknowns leads to the following system of differential equations:

$$\sum_{j=i}^{n_d}\sum_{i=1}^{n_d} a_{ij}\frac{\partial q_j}{\partial x_i} + \sum_{i=1}^{n_d} b_i q_i + cT = g,$$

$$\nabla T - \mathbf{q} = \mathbf{0}, \tag{12}$$

subject to the Dirichlet type boundary conditions as: $T(\mathbf{X}) = \bar{T}(\mathbf{X})$ and $\mathbf{q}(\mathbf{X}) = \bar{\mathbf{q}}(\mathbf{X})$.

The compact form of the equations can be rewritten as:

$$\sum_{i=1}^{n_d} \mathbf{A}_i\frac{\partial \boldsymbol{\varphi}}{\partial x_i} + \boldsymbol{B}\boldsymbol{\varphi} = \mathbf{G}, \qquad \mathbf{G} = [0, 0, ..., 0, g]^T, \tag{13}$$

where $\mathbf{G}$ denotes the vector of right-hand-side and $\boldsymbol{\varphi}$ is the vector of the unknown, defined as:

$$\boldsymbol{\varphi}(\mathbf{X}) = [T_1(\mathbf{X}), T_2(\mathbf{X}), ..., T_i(\mathbf{X}), ..., T_{n_d}(\mathbf{X}), q_1(\mathbf{X}), q_2(\mathbf{X}), ..., q_i(\mathbf{X}), ..., q_{n_d}(\mathbf{X})]^T. \tag{14}$$

$\mathbf{A}_i$ and $\mathbf{B}$ are defined by the following matrices:

$$\mathbf{A}_i = \begin{bmatrix} \delta_{i1} & 0 & 0 & ... & 0 \\ \delta_{i1} & 0 & 0 & 0 & 0 \\ \vdots & \vdots & 0 & \ddots & \vdots \\ \delta_{i1} & 0 & 0 & ... & 0 \\ 0 & a_{i1} & a_{i2} & ... & a_{in_d} \end{bmatrix},$$

$$\delta_{ij} = \begin{cases} 1 & i = j \\ 0 & i \neq j \end{cases}$$

$$\mathbf{B} = \begin{bmatrix} 0 & -1 & 0 & ... & 0 \\ 0 & 0 & -1 & 0 & 0 \\ \vdots & \vdots & 0 & \ddots & \vdots \\ 0 & 0 & ... & 0 & -1 \\ c & b_1 & b_2 & ... & b_{n_d} \end{bmatrix}. \tag{15}$$

By using the MLS approximation, the value of the problem unknown ($\boldsymbol{\phi}$) at an arbitrary collocated point is approximated by Eq. (16), in terms of the unknown nodal parameters ($\hat{\boldsymbol{\phi}}$), as shown in Box I, where nt is the total number of nodes and $N_l(X)$ is the shape function of the l-th node at collocated point $\mathbf{X}$ as defined in Eq. (3). Figure 1 schematically shows collocated and nodal points in an arbitrary support domain.

Similarly, the gradient of the nodal values can be approximated by Eq. (17) as shown in Box II. The residuals of differential equation (R_Ω) and boundary condition (R_Γ) at each collocated point are defined as follows:

$$R_\Omega(\mathbf{X}) = \left(\sum_{i=1}^{n_d} \mathbf{A}_i \frac{\partial \mathbf{M}(\mathbf{X})}{\partial x_i} + \mathbf{B}\mathbf{M}(\mathbf{X}) \right) \hat{\boldsymbol{\varphi}} - \mathbf{G},$$

$$R_\Gamma(\mathbf{X}) = \mathbf{M}(\mathbf{X})\hat{\boldsymbol{\varphi}} - \bar{\boldsymbol{\varphi}}(\mathbf{X}). \tag{18}$$

The least square functional of the residuals is defined

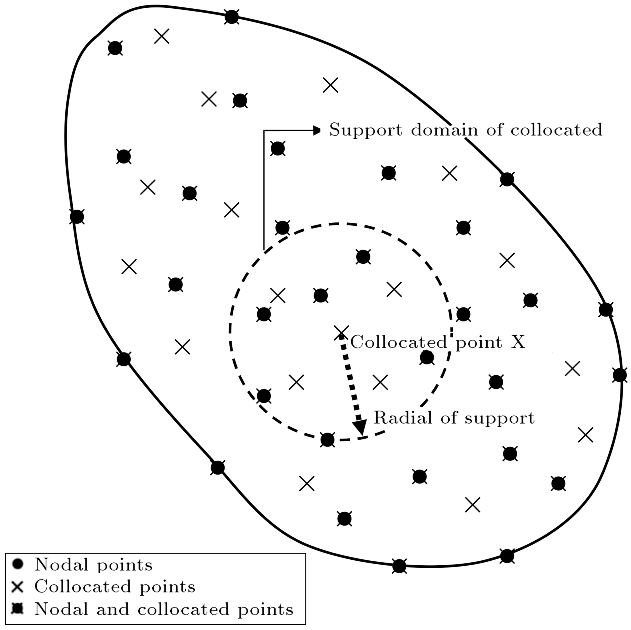

Figure 1. Nodal points and collocated points on an arbitrary support domain.

$$\boldsymbol{\varphi}(\mathbf{X}) = \mathbf{M}(\mathbf{X})\hat{\boldsymbol{\varphi}}; \tag{16}$$

$$\mathbf{M}(\mathbf{X}) = \begin{bmatrix} N_1(\mathbf{X}) & 0 & 0 & ... & N_l(\mathbf{X}) & 0 & 0 & ... & N_{nt}(\mathbf{X}) & 0 & 0 \\ 0 & \ddots & 0 & ... & 0 & \ddots & 0 & ... & 0 & \ddots & 0 \\ 0 & 0 & N_1(\mathbf{X}) & ... & 0 & 0 & N_l(\mathbf{X}) & ... & 0 & 0 & N_{nt}(\mathbf{X}) \end{bmatrix}_{(n_d+1)\times((n_d+1)^* nt)}$$

$$\hat{\boldsymbol{\varphi}} = [\hat{\boldsymbol{\varphi}}(\mathbf{X}_1), \hat{\boldsymbol{\varphi}}(\mathbf{X}_2), \cdots, \hat{\boldsymbol{\varphi}}(\mathbf{X}_i), \cdots, \hat{\boldsymbol{\varphi}}(\mathbf{X}_{nt})]^T,$$

$$\hat{\boldsymbol{\varphi}}(\mathbf{X}_i) = [T(\mathbf{X}_i), q_1(\mathbf{X}_i), \cdots, q_i(\mathbf{X}_i), \cdots, q_{n_d}(\mathbf{X}_i)]^T, \qquad i = 1, 2, \cdots, nt.$$

Box I

$$\frac{\partial \boldsymbol{\varphi}(\mathbf{X})}{\partial x_i} = \frac{\partial \mathbf{M}(\mathbf{X})}{\partial x_i}\hat{\boldsymbol{\varphi}};$$

$$\frac{\partial \mathbf{M}(\mathbf{X})}{\partial x_i} = \begin{bmatrix} \frac{\partial N_1(\mathbf{X})}{\partial x_i} & 0 & 0 & \cdots & \frac{\partial N_{nt}(\mathbf{X})}{\partial x_i} & \cdots & 0 \\ 0 & \ddots & 0 & \cdots & 0 & \ddots & 0 \\ 0 & 0 & \frac{\partial N_1(\mathbf{X})}{\partial x_i} & \cdots & 0 & \cdots & \frac{\partial N_{nt}(\mathbf{X})}{\partial x_i} \end{bmatrix}_{(n_d+1)\times((n_d+1)^* nt)} \qquad i = 1, 2, \cdots, nt. \tag{17}$$

Box II

as follows:

$$\mathrm{Re}=\frac{1}{2}\left(\sum_{i\Omega=1}^{nc}\left(R_\Omega(\mathbf{X}_{i\Omega})\right)^2+\alpha\sum_{i\Gamma=1}^{nb}\left(R_\Gamma(\mathbf{X}_{i\Gamma})\right)^2\right), \tag{19}$$

where $\mathbf{X}_{i\Omega}$ and $\mathbf{X}_{i\Gamma}$ are the coordinates of collocated points arbitrarily distributed over the domain and its boundaries, respectively, nc is the total number of collocated points, and nb is the number of nodes on the boundaries. Here, the penalty method is used to impose the essential boundary conditions with α denoting the penalty coefficient that should be large enough to satisfy the boundary conditions [6,42].

Minimizing Eq. (19) with respect to the unknown nodal parameters leads to:

$$\sum_{i\Omega=1}^{nc}\frac{\partial(R_\Omega(\mathbf{X}_{i\Omega}))}{\partial\hat{\boldsymbol{\varphi}}}(R_\Omega(\mathbf{X}_{i\Omega}))+\alpha\sum_{i\Gamma=1}^{nb}\frac{\partial(R_\Omega(\mathbf{X}_{i\Gamma}))}{\partial\hat{\boldsymbol{\varphi}}}(R_\Omega(\mathbf{X}_{i\Gamma}))=0. \tag{20}$$

Eq. (20) represents a symmetric positive-definite system of linear algebraic equations defined as:

$$\boldsymbol{K}\hat{\boldsymbol{\varphi}}=\mathbf{F}. \tag{21}$$

The coefficient matrix ($\mathbf{K}$) and right-hand-side vector ($\mathbf{F}$) are defined as follows:

$$\mathbf{K}=\sum_{i\Omega=1}^{nc}\mathbf{L}^T(\mathbf{X}_{i\Omega})\mathbf{L}(\mathbf{X}_{i\Omega})+\alpha\sum_{i\Gamma=1}^{nb}\mathbf{M}^T(\mathbf{X}_{i\Gamma})\mathbf{M}(\mathbf{X}_{i\Gamma}),$$

$$\mathbf{L}(\mathbf{X}_{i\Omega})=\sum_{i=1}^{n_d}\mathbf{A}_i\frac{\partial\mathbf{M}(\mathbf{X}_{i\Omega})}{\partial x_i}+\mathbf{B}\mathbf{M}(\mathbf{X}_{i\Omega}), \tag{22}$$

$$\mathbf{F}=\sum_{i\Omega=1}^{nc}\mathbf{L}^T(\mathbf{X}_{i\Omega})\mathbf{G}+\alpha\sum_{i\Gamma=1}^{nb}\mathbf{M}^T(\mathbf{X}_{i\Gamma})\bar{\boldsymbol{\varphi}}(\mathbf{X}_{i\Gamma}), \tag{23}$$

which should be solved for unknown nodal parameters. Since the Kronecker delta function property is not satisfied by the MLS shape function, the nodal parameters are not equal to the nodal values. The nodal values should be retrieved using Eq. (16) [6,42].

In the MDLSM method, collocated points and nodal points are the same. However, in the CMDLSM method, some additional collocated points are used. Since the number of nodal points determines the size of coefficient matrix, the size of the coefficient matrix is not increased by using the additional collocated points. This clearly means that the computational cost for solving the linear algebraic system of equations in the CMDLSM method is the same as that in MDLSM method. However, it is expected that the accuracy of results may be improved by using the CMDLSM method.

In the following, a set of numerical examples is solved to evaluate the performance of the proposed CMDLSM method compared with the MDLSM method.

4. Numerical experiments

In this section, a series of benchmark examples from the literature is used to evaluate the efficiency of the proposed CMDLSM method compared with the MDLSM method. A value of $\alpha = 10^8$ is used for the penalty coefficient. The linear/quadratic basis function is used to construct the MLS shape functions for one/two-dimensional examples. The following error norms are used as the error indicator:

$$\text{error}=\frac{\left\|\mathbf{C}^{\text{exact}}-\mathbf{C}^{\text{numerical}}\right\|_2}{\left\|\mathbf{C}^{\text{exact}}\right\|_2}, \tag{24}$$

where $\mathbf{C}^{\text{exact}}$ and $\mathbf{C}^{\text{numerical}}$ are the vectors of exact and numerical values, respectively, and $||.||$ is the L^2-norm.

4.1. One-dimensional problem

Consider the following one-dimensional equation:

$$\frac{\partial^2 T}{\partial x^2}+\frac{\partial T}{\partial x}=-\sin(x)+\cos(x), \tag{25}$$

where x denotes the coordinate. The Dirichlet type of boundary conditions determined by the exact solution is used to solve the problem. Three sets of uniformly distributed collocated and nodal points are used to solve the problem using MDLSM and CMDLSM methods to study the convergence characteristics of the methods for this problem. Convergence curves are shown in Figure 2 and the error norms of MDLSM and CMDLSM methods are presented in Table 1 for different nodal distributions. The results indicate that the accuracy of solutions is improved by using the

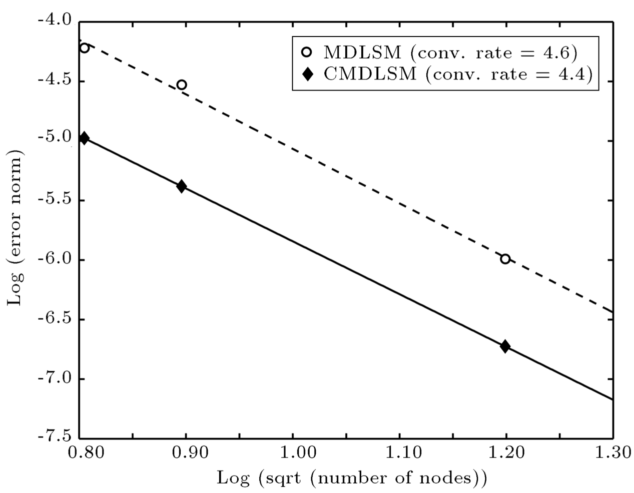

Figure 2. Convergence curves of the MDLSM and CMDLSM methods (first example).

Table 1. Error norms of the MDLSM and CMDLSM results for the first example.

Number of nodes	Number of additional collocated points	MDLSM method	CMDLSM method
5	4	0.0147	0.0069
6	5	0.0108	0.0046
11	10	0.0025	0.0012

Table 2. The effect of the number of additional collocated points on the error norms of CMDLSM for the first example.

Number of additional collocated points	50	100	250	300
Error norm of CMDLSM method	3.9959e-004	1.6469e-004	4.3822e-005	6.3789e-005

additional collocated points. However, the convergence rates of MDLSM and CMDLSM methods are the same. The problem is resolved using different distributions of the additional collocated points with the same number of 11 nodal points, and the results are presented in Table 2, emphasizing the role of additional collocated points for improving the accuracy of the proposed method. Although the obtained results prove the effect of additional collocated points on the accuracy of the proposed method, more studies are required to investigate the best locations of the additional collocated points [41].

4.2. Two-dimensional problem in square domain

In this section, the following two-dimensional PDE is solved:

$$\frac{\partial^2 T}{\partial x^2} + \frac{\partial^2 T}{\partial xy} + \frac{\partial^2 T}{\partial y^2} + (ku^2)T = g(x,y),$$

$$g(x,y) = \left(\left(ku^2 - 2u^2\right)\sin(ux)\cos(uy)\right) - \left(u^2\sin(uy)\cos(ux)\right). \qquad (26)$$

The exact solution to this problem is available as follows:

$$T_{\text{exact}} = \sin(ux)\cos(uy), \qquad (27)$$

where x and y denote the coordinates. Constant coefficients are assumed to be $k = \sqrt{10}$ and $u = 8$, and the problem is solved on a square domain with length one. The Dirichlet type boundary condition of the exact solution is used. First, a set of 121 uniformly distributed nodal points is used to solve the problem using MDLSM method. The same number of nodal points along with 100 additional collocated points is then used to solve the problem using CMDLSM method so that the results can be fairly compared. Using the nodal and collocated points distributions shown in Figure 3, the results of MDLSM and CMDLSM methods are compared on $y = 0.4$ and illustrated in Figure 4. The problem is also solved by the MDLSM method on a uniform distribution of 441 nodal points, and by the CMDLSM on a uniform distribution of 441 nodal points and 400 additional collocated points as shown in Figure 5. Figure 6 compares the results obtained on $y = 0.4$. The error norms of the results produced by the MDLSM and CMDLSM methods

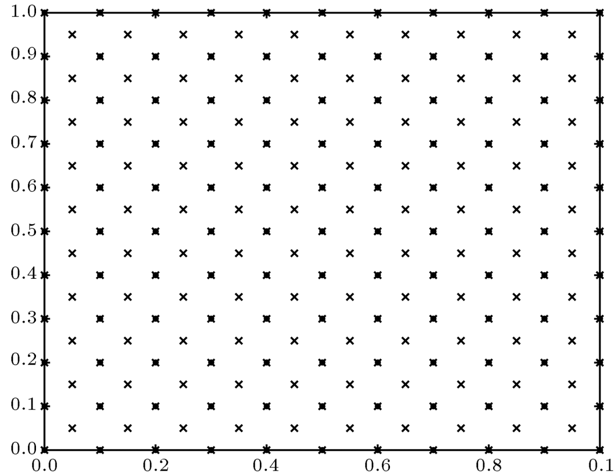

Figure 3. Distribution of 121 nodes and 100 additional collocated points (second example).

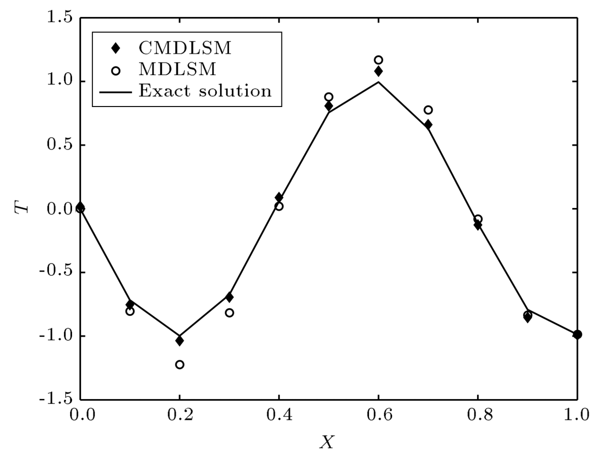

Figure 4. Results of CMDLSM and MDLSM on $y = 0.4$ for 121 nodes and 100 collocated points (second example).

Table 3. Comparison of the errors of MDLSM and CMDLSM methods for the second example.

Number of nodes	Number of additional collocated points	MDLSM method	CMDLSM method
36	25	0.5196	0.4683
121	100	0.1491	0.0681
441	400	0.0401	0.0168

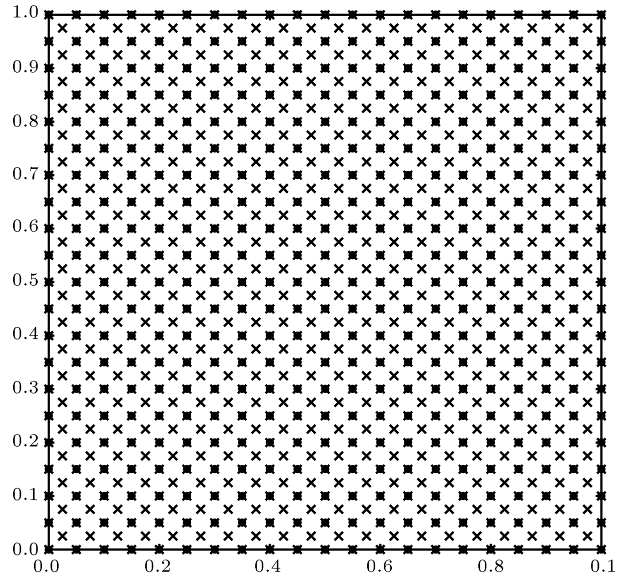

Figure 5. 441 nodes and 400 additional collocated points (second example).

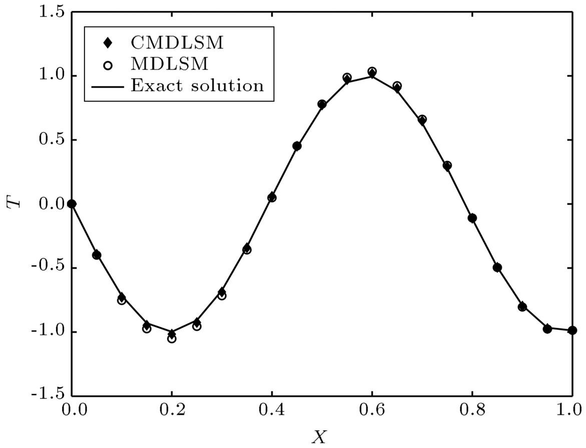

Figure 6. Results of CMDLSM and MDLSM on $y = 0.4$ for 441 nodes and 400 additional collocated points (second example).

are also presented and compared in Table 3. The results clearly show the effect of additional collocated points on the performance of the proposed CMDLSM method. The convergence curves of the MDLSM and CMDLSM methods are compared in Figure 7. Although Figure 7 indicates high rate of convergence for the proposed CMDLSM method compared with

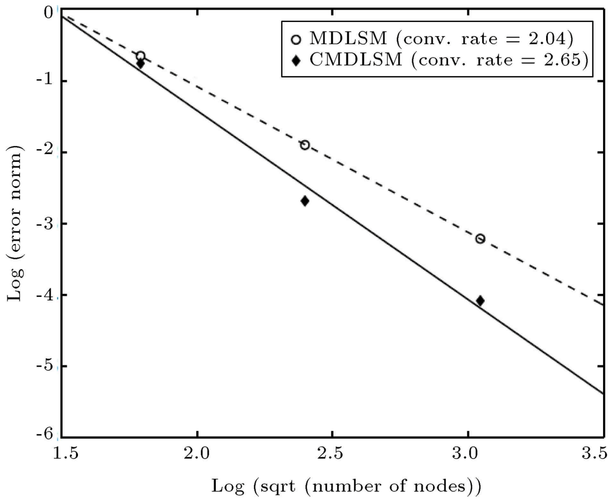

Figure 7. Convergence curves of the MDLSM and CMDLSM methods (second example).

the MDLSM method, the super-convergence of the proposed CMDLSM method cannot be firmly claimed.

4.3. Two-dimensional Laplace problem in circular domain

The following Laplace equation defined on a circular disk with unit radial is solved in this section:

$$\frac{\partial^2 T}{\partial x^2} + \frac{\partial^2 T}{\partial y^2} = 0. \tag{28}$$

The exact solution can be calculated by the following equation [43]:

$$T_{\text{exact}} = r^6 \cos(6\theta), \tag{29}$$

where r is the radial coordinates defining the distance from the center of the circle and θ denotes the polar angle. The Dirichlet type boundary conditions are again used to solve the problem. In this problem, the collocated points are located at the center of Delaunay triangles formed on the nodal points as shown in Figure 8. A set of 102 nodal points along with 169 collocated points as shown in Figure 9 is used to solve the problem by the MDLSM and CMDLSM methods. The contours of results are presented in Figure 10. Another set of 359 nodes and 652 additional collocated points shown in Figure 11 is used to solve the problem with the results compared in Figure 12. Table 4 compares the error norms of the results obtained on different sets of

Table 4. Error norms of the MDLSM and CMDLSM results for the third example.

Number of nodes	Number of additional collocated points	MDLSM method	CMDLSM method
102	169	0.2233	0.1125
359	652	0.0756	0.0395
1345	2561	0.0136	0.0062

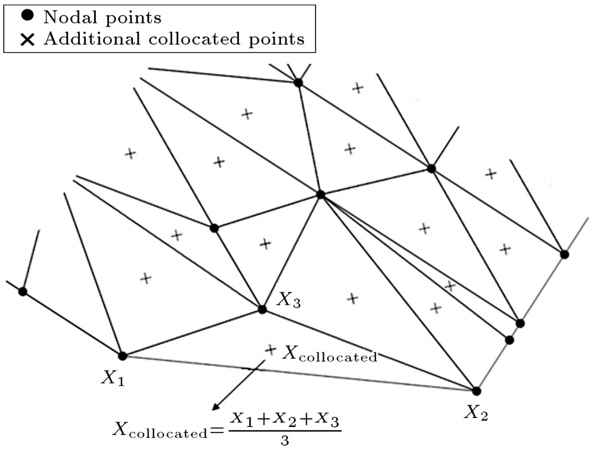

Figure 8. Delaunay triangulation of the nodal points used to locate the additional collocated points.

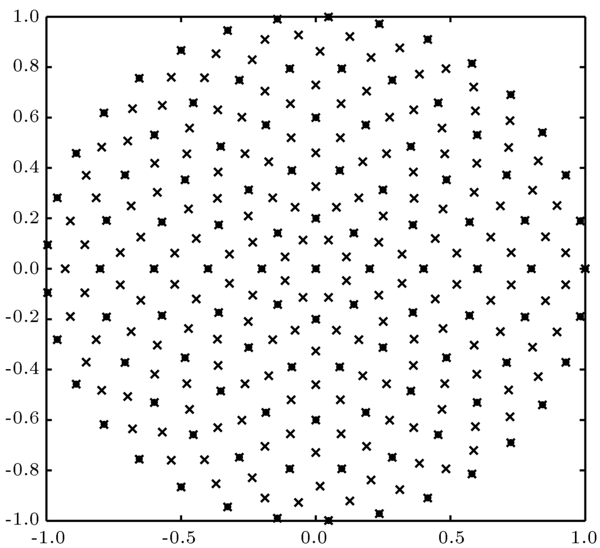

Figure 9. Distribution of 102 nodes and 169 additional collocated points (third example).

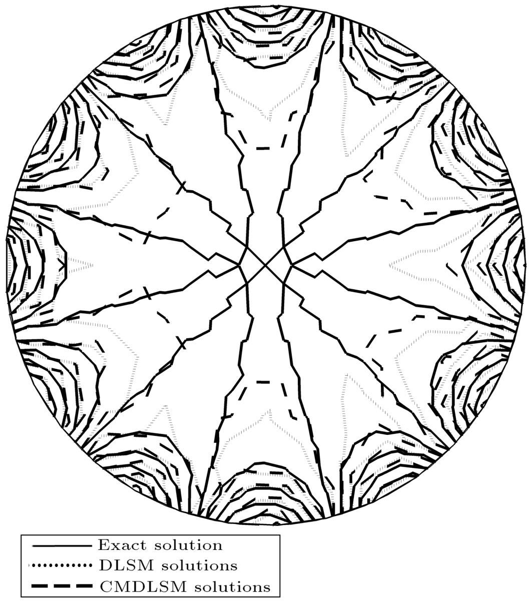

Figure 10. Exact, MDLSM, and CMDLSM solutions for 102 nodes and 169 additional collocated points (third example).

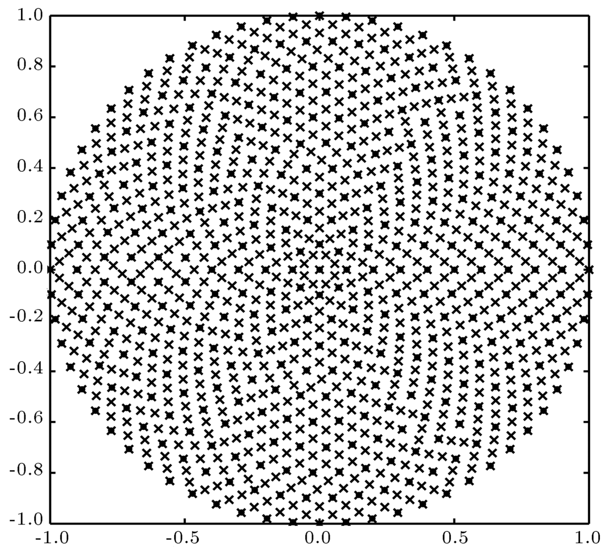

Figure 11. Distribution of 359 nodes and 652 additional collocated points (third example).

nodal distributions. The results indicate considerable improvements in the accuracy of the solutions obtained by the CMDLSM method compared with the MDLSM method. The convergence curves of the MDLSM and CMDLSM methods are also shown in Figure 13.

4.4. Potential flow around a cylinder

Consider the problem of a potential flow around a cylinder of radius R in an infinite domain shown in Figure 14. The governing equation for the problem is:

$$\frac{\partial^2 T}{\partial x^2}+\frac{\partial^2 T}{\partial y^2}=0, \tag{30}$$

where T denotes the stream function. Due to symmetry, the problem is solved on a quarter of the domain,

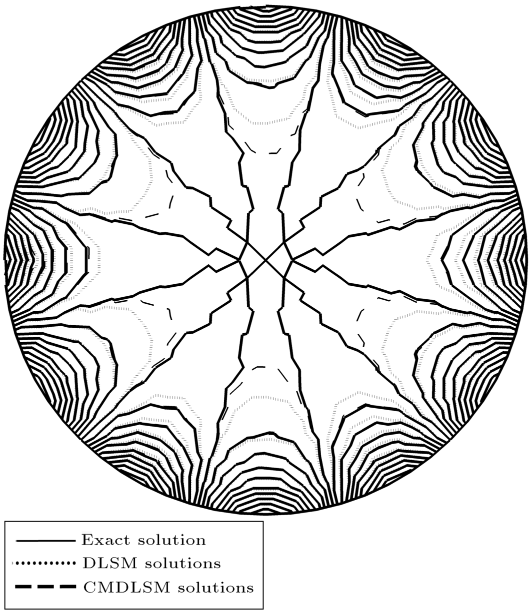

Figure 12. Exact, MDLSM, and CMDLSM solutions for 359 nodes and 652 additional collocated points (third example).

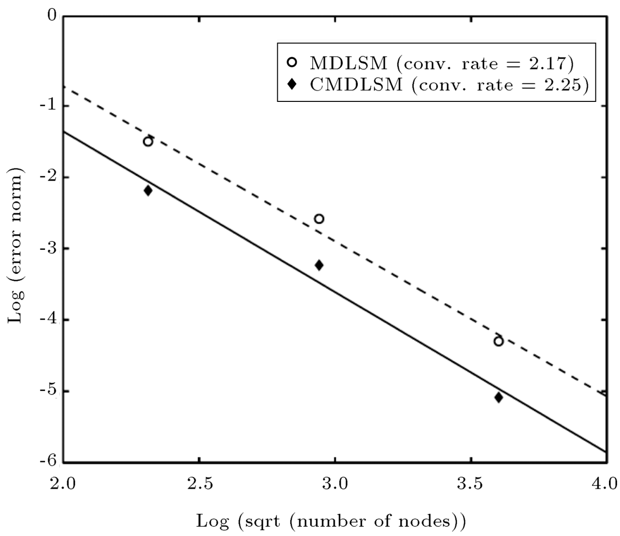

Figure 13. Convergence curves of the MDLSM and CMDLSM methods (third example).

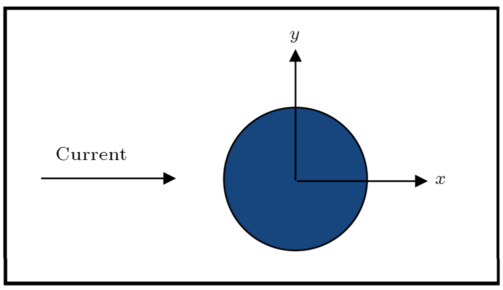

Figure 14. Flow around a cylinder in an infinite domain (fourth example).

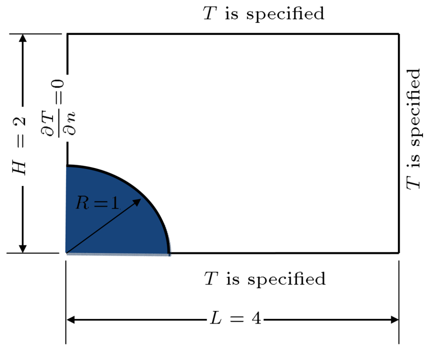

Figure 15. Potential flow problem with boundary conditions (fourth example).

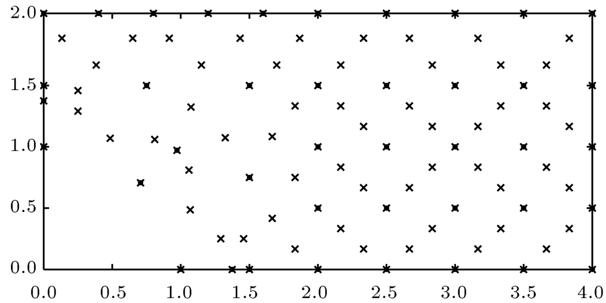

Figure 16. Distribution of 41 nodes and 55 additional collocated points (fourth example).

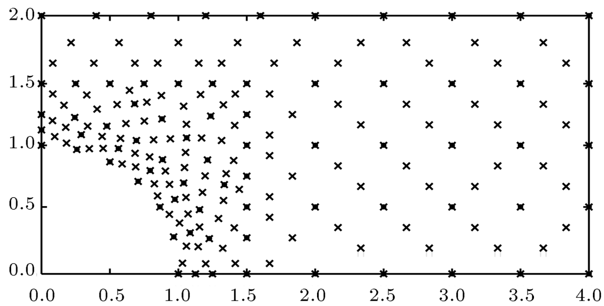

Figure 17. Distribution of 72 nodes and 111 additional collocated points (fourth example).

which is shown in Figure 15. The essential boundary condition of the problem is defined in Figure 15. The exact solution to the problem is available in polar coordinates (r, θ) as follows:

$$T = U\left(r - \frac{R^2}{r}\right)\sin(\theta), \tag{31}$$

where U is a constant parameter assumed to be 1. Similar to the third example, the centers of the Delaunay diagrams are used as the locations of the additional collocated points. Two sets of nodal distributions, shown in Figures 16 and 17, are used to solve the problem with the results compared in Figures 18 and 19. The error norms of the results are compared in Table 5 for the different sets of nodal distributions. The convergence curves of the methods are also shown

Table 5. Error norms of the MDLSM and CMDLSM results for the fourth example.

Number of nodes	Number of additional collocated points	MDLSM method	CMDLSM method
41	55	0.0349	0.0163
47	66	0.0113	0.0081
72	111	0.0055	0.0029

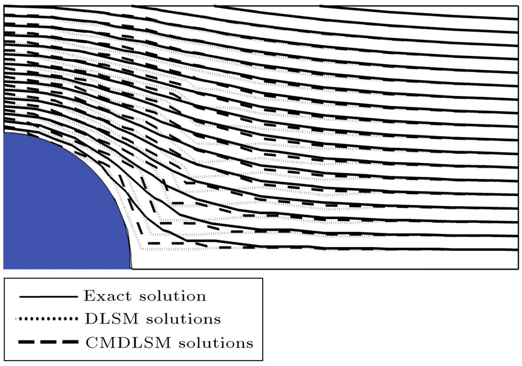

Figure 18. Comparison of the numerical and exact solutions for the distribution of 41 nodes and 56 additional collocated points (fourth example).

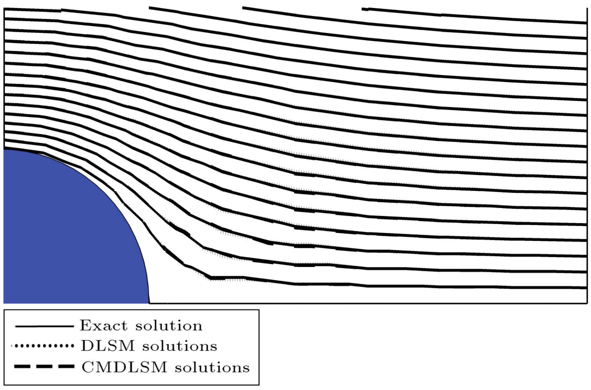

Figure 19. Comparison of the numerical and exact solutions for the distribution of 72 nodes and 111 additional collocated points (fourth example).

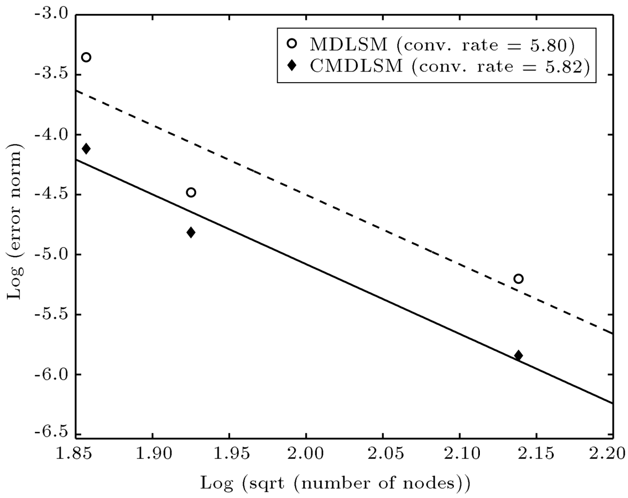

Figure 20. Convergence curves of the MDLSM and CMDLSM methods (fourth example).

in Figure 20. The results clearly indicate the positive role of additional collocated points in the proposed CMDLSM method to produce more accurate results than the results of the MDLSM method.

5. Conclusion

In this paper, a CMDLSM method was proposed and used to attain an efficient solution to engineering problems. As the background mesh is not required in the MDLSM method, it is a truly meshless method. The method circumvents the Ladyzenskaja-Babuska-Brezzi (LBB) condition due to the use of least squares concept, leading to symmetric and positive-definite system of equations. Nodal points were used in the MDLSM methods to construct the shape functions, while collocated points were used to form the least squares functional. In the original MDLSM method, the location of the nodal points and collocated points is the same. In the proposed CMDLSM method, a set of additional collocated points was introduced. A set of benchmark numerical examples, cited in the literature, was used to evaluate the performance of the proposed method. Applying the proposed CMDLSM method to the engineering problems showed that the accuracy of results was notably improved by using the additional collocated points. More studies are required to find the best location of the additional collocated points. It is noted that the size of coefficient matrix was not increased in the proposed CMDLSM method and, therefore, the required computational effort for solving the linear algebraic system of equations was the same as that in the MDLSM method.

References

1. Eymard, R., Gallouöt, T., and Herbin, R. "Finite volume methods", *Handbook of Numerical Analysis*, **7**, pp. 713-1018 (2000).
2. Reddy, J.N., *An Introduction to the Finite Element Method*, **2**, McGraw-Hill, New York (1993).
3. De Sciarra, F.M. "A nonlocal finite element approach to nanobeams", *Advances in Mechanical Engineering*, **5**, p. 720406 (2013).

4. De Sciarra, F.M. "Finite element modelling of nonlocal beams", *Physica E: Low-Dimensional Systems and Nanostructures*, **59**, pp. 144-149 (2014).

5. De Sciarra, F.M. "Variational formulations, convergence and stability properties in nonlocal elastoplasticity", *International Journal of Solids and Structures*, **45**(7), pp. 2322-2354 (2008).

6. Liu, G.-R., *Meshfree Methods: Moving Beyond the Finite Element Method*, Taylor & Francis (2009).

7. Liu, G.-R. and Nguyen, T.T., *Smoothed Finite Element Methods,* CRC Press (2010).

8. Xue, B., Wu, S., Zhang, W., and Liu, G. "A smoothed FEM (S-FEM) for heat transfer problems", *International Journal of Computational Methods*, **10**(01), p. 1340001 (2013).

9. Li, W., Chai, Y., Lei, M., and Liu, G. "Analysis of coupled structural-acoustic problems based on the smoothed finite element method (S-FEM)", *Engineering Analysis with Boundary Elements,* **42**, pp. 84-91 (2014).

10. Liu, G., Dai, K., and Nguyen, T. "A smoothed finite element method for mechanics problems", *Computational Mechanics*, **39**(6), pp. 859-877 (2007).

11. Chen, Z., Zong, Z., Liu, M., Zou, L., Li, H., and Shu, C. "An SPH model for multiphase flows with complex interfaces and large density differences", *Journal of Computational Physics*, **283**, pp. 169-188 (2015).

12. Canelas, R.B., Crespo, A.J., Domínguez, J.M., Ferreira, R.M., and Gómez-Gesteira, M. "SPH-DCDEM model for arbitrary geometries in free surface solid-fluid flows", *Computer Physics Communications*, **202**, pp. 131-140 (2016).

13. Koshizuka, S., Nobe, A., and Oka, Y. "Numerical analysis of breaking waves using the moving particle semi-implicit method", *International Journal for Numerical Methods in Fluids*, **26**(7), pp. 751-769 (1998).

14. Khanpour, M., Zarrati, A.R., Kolahdoozan, M., Shakibaeinia, A., and Jafarinik, S. "Numerical modeling of free surface flow in hydraulic structures using Smoothed Particle Hydrodynamics", *Applied Mathematical Modelling*, **40**(23-24), pp. 9821-9834 (December 2016).

15. Shakibaeinia, A. and Jin, Y.-C. "MPS mesh-free particle method for multiphase flows", *Computer Methods in Applied Mechanics and Engineering*, **229**, pp. 13-26 (2012).

16. Khayyer, A. and Gotoh, H. "Modified moving particle semi-implicit methods for the prediction of 2D wave impact pressure", *Coastal Engineering*, **56**(4), pp. 419-440 (2009).

17. Chen, W.-H. and Guo, X.-M. "Element free Galerkin method for three-dimensional structural analysis", *Computer Modeling in Engineering and Sciences,* **2**(4), pp. 497-508 (2001).

18. Zhang, Z., Liew, K.M., Cheng, Y., and Lee, Y. "Analyzing 2D fracture problems with the improved element-free Galerkin method", *Engineering Analysis with Boundary Elements,* **32**(3), pp. 241-250 (2008).

19. Singh, A., Singh, I.V., and Prakash, R. "Meshless element free Galerkin method for unsteady nonlinear heat transfer problems", *International Journal of Heat and Mass Transfer*, **50**(5), pp. 1212-1219 (2007).

20. Atluri, S., Liu, H., and Han, Z. "Meshless local Petrov-Galerkin (MLPG) mixed collocation method for elasticity problems", *CMC-TECH Science Press-*, **4**(3), p. 141 (2006).

21. Lin, H. and Atluri, S. "The meshless local Petrov-Galerkin (MLPG) method for solving incompressible Navier-stokes equations", *CMES-Computer Modeling in Engineering and Sciences*, **2**(2), pp. 117-142 (2001).

22. Najafi, M., Arefmanesh, A., and Enjilela, V. "Meshless local Petrov-Galerkin method-higher Reynolds numbers fluid flow applications", *Engineering Analysis with Boundary Elements*, **36**(11), pp. 1671-1685 (2012).

23. Onate, E. and Idelsohn, S. "A mesh-free finite point method for advective-diffusive transport and fluid flow problems", *Computational Mechanics*, **21**(4-5), pp. 283-292 (1998).

24. Shojaei, A., Mudric, T., Zaccariotto, M., and Galvanetto, U. "A coupled meshless finite point/Peridynamic method for 2D dynamic fracture analysis", *International Journal of Mechanical Sciences*, **119**, pp. 419-431 (2016).

25. Resöndiz-Flores, E.O. and Saucedo-Zendejo, F.R. "Two-dimensional numerical simulation of heat transfer with moving heat source in welding using the finite pointset method", *International Journal of Heat and Mass Transfer*, **90**, pp. 239-245 (2015).

26. Liu, X., Liu, G., Tai, K., and Lam, K. "Radial point interpolation collocation method (RPICM) for partial differential equations", *Computens & Mathematics with Applications*, **50**(8), pp. 1425-1442 (2005).

27. Mohebbi, A., Abbaszadeh, M., and Dehghan, M. "The use of a meshless technique based on collocation and radial basis functions for solving the time fractional nonlinear Schrödinger equation arising in quantum mechanics", *Engineering Analysis with Boundary Elements*, **37**(2), pp. 475-485 (2013).

28. Liu, X., Liu, G., Tai, K., and Lam, K. "Radial point interpolation collocation method (RPICM) for the solution of nonlinear Poisson problems", *Computational Mechanics*, **36**(4), pp. 298-306 (2005).

29. Cheng, M. and Liu, G. "A novel finite point method for flow simulation", *International Journal for Numerical Methods in Fluids*, **39**(12), pp. 1161-1178 (2002).

30. Liu, G., Kee, B.B., and Chun, L. "A stabilized least-squares radial point collocation method (LS-RPCM) for adaptive analysis", *Computer Methods in Applied Mechanics and Engineering*, **195**(37), pp. 4843-4861 (2006).

31. Kee, B.B., Liu, G., and Lu, C. "A least-square radial point collocation method for adaptive analysis in linear elasticity", *Engineering Analysis with Boundary Elements*, **32**(6), pp. 440-460 (2008).

32. Kee, B.B., Liu, G., and Lu, C. "A regularized least-squares radial point collocation method (RLS-RPCM) for adaptive analysis", *Computational Mechanics*, **40**(5), pp. 837-853 (2007).

33. Kee, B.B., Liu, G., Zhang, G., and Lu, C. "A residual based error estimator using radial basis functions", *Finite Elements in Analysis and Design,* **44**(9), pp. 631-645 (2008).

34. Afshar, M., Amani, J., and Naisipour, M. "A node enrichment adaptive refinement in discrete least squares meshless method for solution of elasticity problems", *Engineering Analysis with Boundary Elements*, **36**(3), pp. 385-393 (2012).

35. Kazeroni, S.N. and Afshar, M. "An adaptive node regeneration technique for the efficient solution of elasticity problems using MDLSM method", *Engineering Analysis with Boundary Elements*, **50**, pp. 198-211 (2015).

36. Shobeyri, G. and Afshar, M. "Corrected discrete least-squares meshless method for simulating free surface flows", *Engineering Analysis with Boundary Elements*, **36**(11), pp. 1581-1594 (2012).

37. Shobeyri, G. and Afshar, M. "Adaptive simulation of free surface flows with discrete least squares meshless (DLSM) method using a posteriori error estimator", *Engineering Computations*, **29**(8), pp. 794-813 (2012).

38. Faraji, S., Afshar, M., and Amani, J. "Mixed discrete least square meshless method for solution of quadratic partial differential equations", *Scientia Iranica*, **21**(3), pp. 492-504 (2014).

39. Amani, J., Afshar, M., and Naisipour, M. "Mixed discrete least squares meshless method for planar elasticity problems using regular and irregular nodal distributions", *Engineering Analysis with Boundary Elements*, **36**(5), pp. 894-902 (2012).

40. Faraji, S., Kolahdoozan, M., and Afshar, M. "Mixed discrete least squares meshless method for solving the linear and non-linear propagation problems", *Scientia Iranica*, **25**(2), pp. 565-578 (2018).

41. Firoozjaee, A.R. and Afshar, M.H. "Discrete least squares meshless method with sampling points for the solution of elliptic partial differential equations", *Engineering Analysis with Boundary Elements*, **33**(1), pp. 83-92 (2009).

42. Liu, G.-R. and Gu, Y.-T., *An Introduction to Meshfree Methods and Their Programming*, Springer Science & Business Media (2005).

43. Liu, Y. "A new boundary meshfree method with distributed sources", *Engineering Analysis with Boundary Elements*, **34**(11), pp. 914-919 (2010).

Biographies

Saeb Faraji Gargari received his BSc form the Department of Civil Engineering, Urmia University, and his MSc in Structural and Hydraulic Engineering from Iran University of Science and Technology. He is now PhD student at Amirkabir University of Technology. His research interests include improving and developing the meshless numerical methods for solving the Partial Differential Equations (PDEs), and governing the engineering problems.

Morteza Kolahdoozan received his BSc from the Department of Civil Engineering, Amirkabir University of Technology, MSc degree from the Department of Civil Engineering, Tehran University, and PhD degree from the University of Bradford, UK. He is now Associate Professor of the Department of Civil and Environmental Engineering, Amirkabir University of Technology, Tehran, Iran. His research interests include numerical and physical simulation of the fluid mechanics problems. The emphasis of his research is on coastal hydrodynamics, sediment transport, and oil propagation.

Mohammad Hadi Afshar obtained his BS degree in Civil Engineering from Tehran University and his MS and PhD degrees from University College of Swansea. He is now Associate Professor in Civil Engineering Department at Iran University of Science and Technology. His research interests include numerical modeling of elasticity and fluid mechanics problems, especially by using the meshless methods and optimization.